

Effects of corrosion on a steel bowstring bridge in marine environment: a case-study of assessment and retrofit

Michele Fabio Granata^{1*}

Abstract

The case-study of a steel bowstring bridge set in a marine environment and highly damaged by corrosion is presented. The bridge was built in 2004 and was repainted for corrosion protection in 2010. Despite the recent construction and the maintenance interventions, many structural elements like hangers are highly damaged by corrosion with decreasing performance in terms of serviceability and ultimate limit states. A deep investigation was carried out in order to assess the bridge and to establish the necessary retrofit actions to be carried out in the near future. In-situ tests reveal the reduced performance of the original steel in terms of strength and corrosion protection, together with the inefficiency of the successive maintenance interventions. For this reason the author made drastic choices for assessing the bridge and for its retrofit, down to replacement of hangers and entire galvanization through thermal spray coating technology, in order to increase the expectations of durability in service life. The results of the investigations carried out on the bridge as well as the choices of intervention are presented and discussed.

Keywords: arch, tie, bowstring bridge, corrosion, steel bridge, hangers

Introduction

The corrosion of steel bridges in a marine environment is a challenge to the bridge engineer because many existing bridges show that the development of corrosion in steel members is more rapid than expected, even in the case in which the maintenance interventions of the owner are regular; when maintenance action is not regularly applied or it does not achieve the expected effectiveness, a decreasing performance occurs in terms of serviceability and in the extreme cases the ultimate limit state could be reached in the most stressed elements.

In its simplest form, corrosion of steel results from exposure to oxygen and moisture. Corrosion is accelerated in the presence of salt from roadway deicing, salt water, or perhaps salt deposited from other sources. Although steel corrodes readily in the presence of oxygen and moisture, the rate of corrosion is accelerated in the presence of chloride ions or other corrosive chemicals. Chloride ions result mainly

¹ Università di Palermo, Dipartimento di Ingegneria, Palermo, Italy

*Corresponding author. Researcher, PhD, PE, M.ASCE. e-mail: michelefabio.granata@unipa.it

33 from the use of deicing agents composed of materials with readily soluble chloride ions. These ions
34 create an atmosphere in which unprotected steel corrodes very quickly. In order to improve durability,
35 paintings are used as coatings for protecting steel from the impact of the environment [1]. Particularly,
36 seawater consists of a solution of many salts and numerous organic and inorganic particles in suspension.
37 Its main characteristics are salinity and chlorinity and, from the corrosion point of view, dissolved
38 oxygen content, which ranges from 4 to 8 mg/l, depending on temperature and depth. Its minor
39 components include dissolved gases – CO₂, NH₃ and H₂S – found in seawater contaminated by urban
40 sewage or due to algae, bacteria, etc. [2]. An interesting review on steel corrosion in marine
41 environments is reported by Alcantara et al. [3]. Steel bridge corrosion prevention and mitigation
42 strategies are reported in Stephens et al. [4] while Kreislova and Geiplova [5] give useful indications on
43 the evaluation of coatings for steel protection.

44 In this paper a case-study of a steel tied-arch bridge, known also as a bowstring bridge [6,7], with two
45 inward inclined arches, in Southern Italy, over the mouth of a river, is presented and discussed. The
46 main cause of the high corrosion level was the original lack of steel galvanization, because the designer
47 was confident in a coating system composed only of an external epoxy-based painting. The damage due
48 to corrosion is mainly concentrated in the hangers, whose cross-section was reduced with respect to the
49 original one, with the danger of achievement of the local conditions for failure. The choices made by
50 the author for the retrofit interventions are presented: particularly the replacement of hangers and a new
51 strategy for coating and corrosion protection including thermal spray zinc coating in a duplex-kind
52 coating with three-layer painting.

53

54 **1 Geometry of the case-study bridge**

55 The case-study is an existing arch bridge with inward arches in Sicily, over the mouth of the river Arena
56 in Mazara del Vallo, along the seafront of the town.

57 The upper arch is composed of two arches, inclined inward by 18°. The arch cross-section is a steel
58 box 700x900 mm. The two arches are stiffened by 11 transverse beams. The bridge has longitudinal and
59 transverse symmetry with 27 hangers at each bridge side for a total number of 54 hangers made of
60 circular steel bars, 70 mm in diameter. The deck is composed of two longitudinal side beams, with
61 double T section, 900 mm wide and 1750 mm high, which are extradosed with respect to the platform
62 and inclined 18°, lying in the same plane as the arches and hangers. The longitudinal beams are stiffened
63 by transverse double T beams 800 mm high with L diagonal bracing and an upper reinforced concrete
64 slab 25 mm thick. The upper slab is connected only to the transverse beams through Nelson rods, but
65 not to the longitudinal ones, which are almost independent and linked only to the steel elements of arch,
66 hangers and deck. The deck supports a single carriageway and two side footways. The total length of
67 the bridge is 87 m, and the span between supports is 85.4 m. The arch rise is 16.5 m ($f/l = 0.193$) and
68 the hanger spacing is 3.05 m. Each abutment is founded on 8 piles with diameter 1.20 m. The geometry

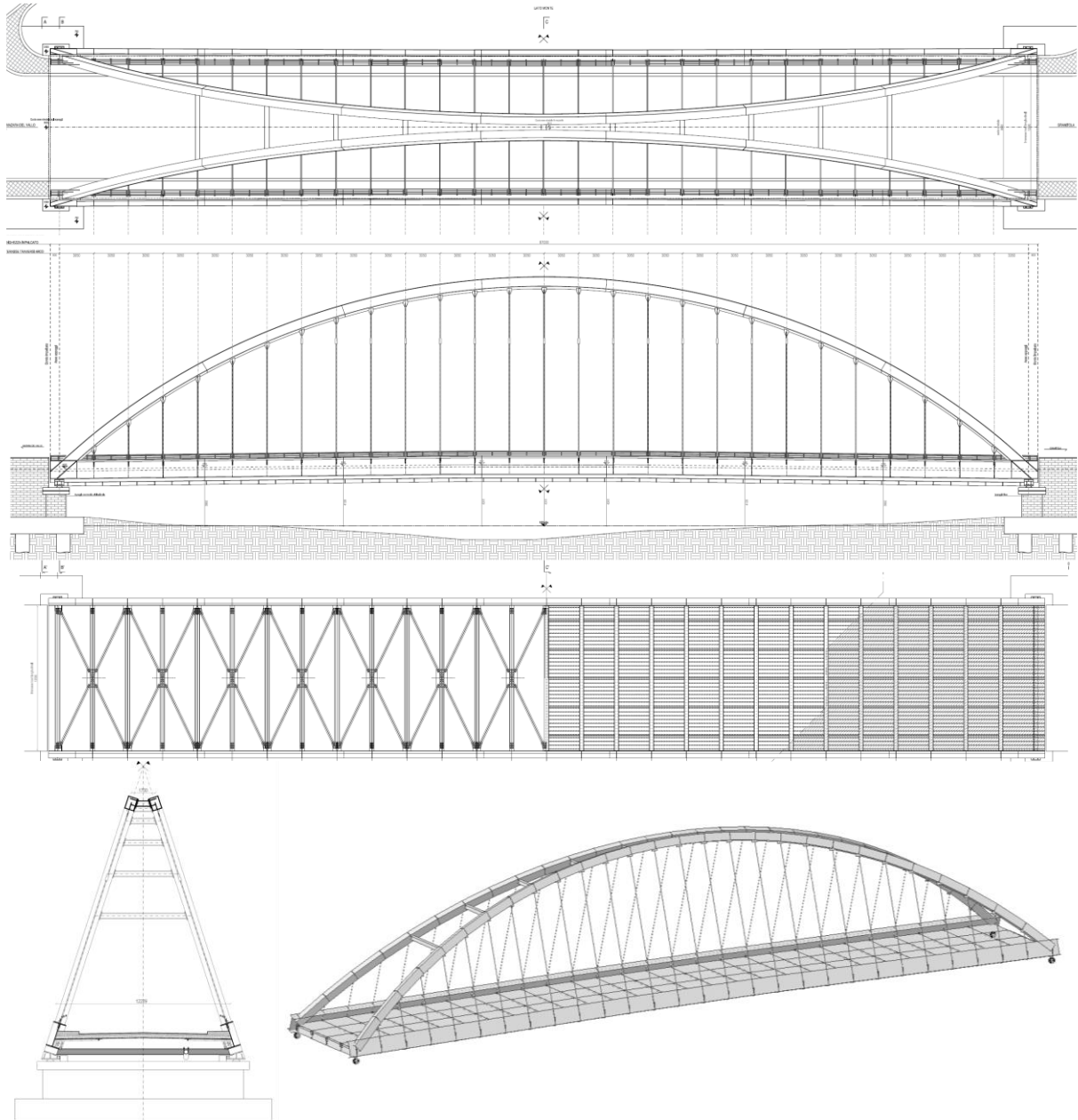
69 is shown in figure 1. Pictures of the bridge environment are shown in figure 2.
70 The design tensile yield strength of the steel is $f_{yk} = 355$ MPa and the concrete strength is $f_{ck} = 35$ MPa.
71 The elastic modulus of the concrete $E_c = 30500$ MPa and the elastic modulus of the steel $E_s = 210000$
72 MPa.

73

74

75

76



77

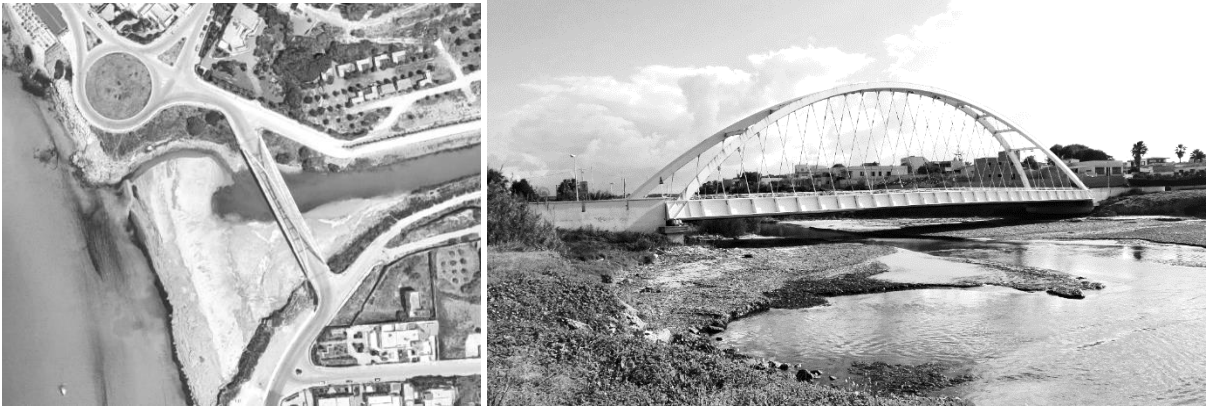
78

79

Figure 1. Geometry of the case-study bridge

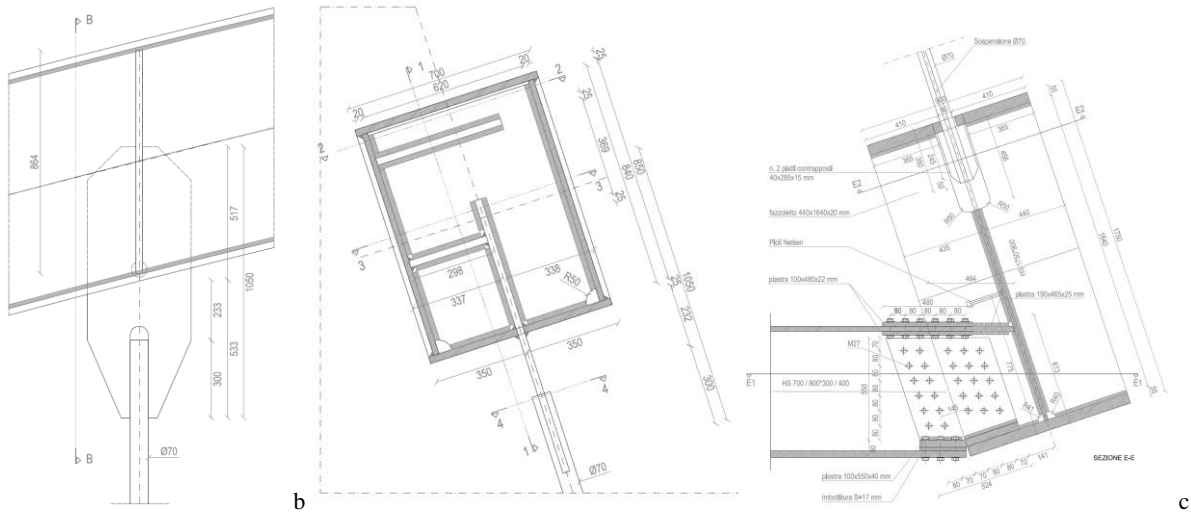
80 An important characteristic of the bridge is that the hangers are made of steel bars with couplers for bars
81 longer than 12 m; the connections welded to the arch and deck main beam are the critical points for
82 corrosion and local damage together with the couplers. This kind of connections does not allow for
83 hangers re-tensioning and/or simple replacement and it was the main difficulty to be faced for the retrofit
84 design (fig. 3).

85



86
87
88

Figure 2. Aerial and perspective views of the bridge environment



89

a b c



90

d

91
92
93
94

Figure 3. Hanger attachment joints (welded connections) to the arch (a,b) and to the main beam (c). Views of corroded hangers and attachment joints (d)

95 **2 Bridge assessment and onsite test evaluation**

96 The outcome of the in-situ investigations and laboratory tests made it possible to determine the strength
97 of the main elements, their degree of corrosion and damage as well as the high average rate of corrosion
98 and the actual effectiveness of the maintenance intervention previously put in place. From these results
99 it is clear that the most stressed and damaged elements are the hangers and especially those over 12 m
100 long which have a bar coupler (fig. 4). Visual and instrumental investigations agree in diagnosing a
101 reduction of cross-section in many hangers, especially at the base, in the hole of the principal beam
102 which allows the hanger bar to go down and to be welded at the centroid of the steel beam (fig. 3d).
103 Moreover, many other areas of water stagnation present a high rate of corrosion: couplers, areas for
104 attaching road signs on the hangers, etc.

105



106
107
108
109

Figure 4. Pictures of hanger corrosion: bar coupler and upper joint welded to the arch



110
111
112
113

Figure 5. Pictures of member corrosion: joint of hangers to the principal beam, pitting in the principal beam, transverse beam bolt connection

114 Corrosion is also localized in some areas of the beam (inner edge of the upper flange, attachment
115 areas of the hangers, lower transverse beams and bolted connections, etc.) and of the arch (connections
116 with the transverse beams, drains on the inner area and outside of the web). In some points, pitting
117 phenomena were detected, i.e. very localized corrosion that goes deep inside the steel section, compared
118 to the surrounding areas [8].

119 The deterioration of structural elements is mainly caused by corrosion in the marine environment. In
120 this specific case, the high rate of corrosion is the essential element to be faced in the assessment because
121 after fifteen years of life the bridge shows signs of serious damage, especially for the hangers, despite
122 the fact that maintenance has already been carried out. Corrosion proceeds in these elements very
123 quickly, even under the skin, that is, under the detached coating, with inhomogeneity on the surface, and
124 concentration of deep corrosion in some points up to pitting phenomena (fig. 5), exfoliation and fractures
125 with reductions of steel cross section.

126 Atmospheric corrosion occurs in the layer of humidity on the metal surface, often not visible to the
127 naked eye, and the rate of corrosion is also affected by various factors such as relative humidity,
128 condensation and the increase in the rate of pollution in the atmosphere. In this case the presence of
129 rotting algae (with probable sulfate-reducing bacteria) could be an accelerating factor, together with the
130 high humidity and average temperature [2,9].

131 In order to correctly assess this situation, it was necessary to identify and classify the corrosiveness
132 of the environment in the area where the structure is located and the consequent identification of the
133 durability of the corrosion protection systems according to the type of coating chosen.

134 From the investigations carried out, it appears that the bridge, despite being in an area with high
135 susceptibility to corrosion, has not undergone galvanizing treatments during construction, hence
136 protection has always been entrusted (starting from the original project) to epoxy-based painting cycles.
137 Since durability is the expected time of duration of the effectiveness of an anticorrosive protection until
138 the first important maintenance intervention, this is a case of very low durability: 5 years of life before
139 the intervention made in 2010 and 15 years of life at present with the need for a major maintenance
140 intervention, less than ten years from the first.

141 In the following sections the investigations carried out on the bridge and their results are discussed,
142 highlighting the most important elements for assessment. Investigations were carried out with dynamic
143 tests on the hangers and bridge deck; samples of steel elements being taken from various structural
144 members for direct tensile tests (strength determination), hardness and resilience tests in the laboratory,
145 as well as for performing chemical-metallographic tests and microscope investigations; in-situ hardness
146 tests; thickness of the elements and protective coating; combined visual, magnetoscopic and ultrasonic
147 investigations on welded and bolted joints. Investigations are carried out by the author in cooperation
148 with 4EMME Service s.p.a., national test laboratory authorized by the Italian Ministry of Infrastructures
149 for on-site investigations and laboratory tests on structures and specialized on bridges.

150

2.1 Material testing, steel corrosion and metallographic investigation

2.1.1 Coating thickness

The coating thickness values were measured on all the samples of structural elements. Very variable values of the coating thickness were found from a minimum of 542 μm to a maximum of 1181 μm above a hanger, a value which is however considered misleading as detachment from the support by internal oxidation of the hanger may have led to an alteration of the measures. An average value of about 700 μm is therefore believed to be likely, which is quite high compared to the ordinary values of the in-situ paints. Of course, it should be considered that the intervention, carried out in 2010 with epoxy paints of the Surface Tolerant type, is mostly superimposed on the previous one, because it was only done with water cleaning of the surfaces and without sandblasting. For this reason, although the detected thickness of the coating is considerable, it does not seem that it was effective for protection from corrosion, especially in the points where the marine aerosol has most attacked the structural elements due to the persistence of water, favored by the prevailing winds (joints, surfaces and base of the hangers, couplers, edge of the beam and arch inclined inwards, etc.).

Metallographic analyses were carried out under a microscope on samples taken onsite.

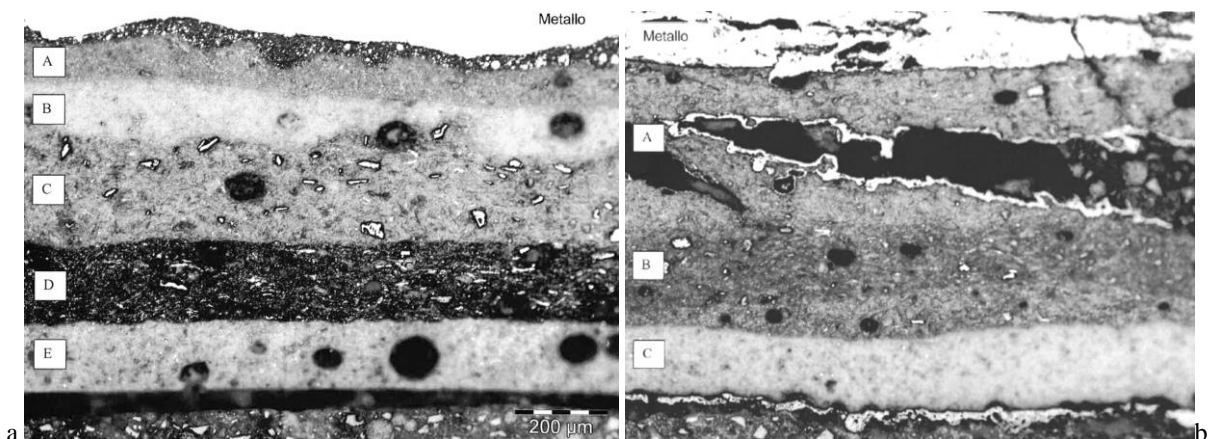


Figure 6. Microscope sections (100X) of two samples: a) deck beam; b) hanger

The results of the samples always show five different coating layers indicated with the letters A to E starting from the steel towards the outside (fig. 6a). Layer A is always an attack; in general it appears that the first three layers A, B, C refer to the period of construction, and the layers D and E to a later period, referable to the maintenance intervention carried out in 2010. The thickness of layers A and B is always around 100 μm , layer C doubles to about 200 μm , and layers D and E are instead about 140 μm thick each. The overall thickness of the coating package is approximately 700 μm , compatible with the average of the coating thicknesses detected by the in-situ tests. Evidently in these cases, the 2010 intervention only cleaned the surfaces of the previous coating and the epoxy-based Surface Tolerant paints overlapped those already present; here when layers are well bounded, the steel is well protected from corrosion. No traces of previous galvanizing layers were detected.

The result of the hanger samples instead shows 3 layers (fig. 6b):

- the inner layer is indicated by A and it is very thick (about 350 μm) with showy inclusions of oxides, hence it refers to the three original layers detected in the other samples covered in turn by the post-construction intervention. Here the painting was carried out on an already oxidized surface, in the absence

183 of a thorough cleaning of the steel support, or without sandblasting.

184 - The outer layers B and C are therefore attributable to the maintenance intervention carried out in 2010.
185 Unfortunately, the investigation on the hanger shows that the cleaning was not thoroughly carried out; hence the
186 application of the paints included the oxidized layer and the progression of corrosion continued in time. This may
187 explain the advanced state of corrosion suffered by the hangers compared to other elements.

188

189 **2.1.2 Steel member thickness**

190 As for the thickness of the steel elements, it was detected by means of an ultrasonic thickness gauge, after cleaning
191 the investigation surfaces. The investigated thickness concerned the arch and deck sections (flanges and webs) and
192 the residual thickness of the hangers in the areas that appeared most oxidized and easily accessible during on-site
193 operations. The results confirm the geometry of the steel plates of the original design and of the accounting
194 drawings.

195 As for the hangers, while in the still intact areas, hanger diameters equal to 70 mm were found, and therefore, in
196 line with the original nominal diameter, the measurements made in the corroded areas showed major section
197 reductions for significant extensions and on many hangers. The average value of the section reduction is 5.5 mm
198 (residual diameter 64.5 mm) which corresponds to a reduction of 7.78% in terms of diameter, 14.95% in terms of
199 area and 21.56% in terms of strength modulus of the cross-section. The most corroded hangers show section
200 reductions of almost 10 mm in diameter with area reductions of more than 24% and strength modulus reductions
201 of over 34%.

202

203 **2.1.3 Tensile steel strength and hardness**

204 The hardness tests were carried out in a diffuse way on all the elements in situ by means of a portable hardness
205 tester and in the laboratory, on the steel samples taken for the tensile break test. A more extensive campaign was
206 repeated on the hangers after the results of the first tests had been acquired (HB = Brinell hardness).

207 The average of the hardness on the lower transverse beams of the deck was HB = 166 corresponding to an
208 equivalent steel strength of $f_t = 556$ MPa, in line with a S355 grade steel.

209 The average of the hardness on the principal beam of the deck beams was HB = 135 corresponding to an equivalent
210 steel strength of $f_t = 452$ MPa, not compatible with a S355 grade steel but with a S275 grade steel.

211 The average of the hardness on the steel members of the arch was HB = 144 corresponding to an equivalent steel
212 strength of $f_t = 482$ MPa, not compatible with a S355 grade steel but with a S275 grade steel.

213 The average of the hardness on the hangers was HB = 127 corresponding to an equivalent steel breaking tension
214 of $f_t = 424$ MPa, not compatible with a S355 grade steel but, at the limit, with a S355 grade steel but with a S275
215 grade steel. It is worth noting that many values of hardness onsite are below a S275 grade for hangers, down to the
216 minimum value of HB = 115, corresponding to a steel strength of $f_t = 380$ MPa.

217 By using the direct tensile strength test for calibration of the correlation coefficient between the hardness measured
218 in the laboratory and those obtained in situ, the result is an average correlation coefficient $f_t/HB = 3.35$, which
219 confirms the value of the literature curve adopted for the hardness tester in situ. The hardness-strength correlation
220 is therefore confirmed by laboratory tests and the correlation coefficient is in the range suggested by the Standard
221 ASTM A370, which reports a table of correlation between hardness and steel strength [10]. From this table the
222 current range of values for S275 grade steel is HB = 125÷140 ($f_t=430$ MPa) while for S355 grade steel is HB =
223 150÷165 ($f_t=510$ MPa).

224 Regarding the tensile strength values determined by direct laboratory tests, they confirm the indirect evaluations
225 made through the hardness test campaign.

226

227 **2.1.4 Tests on welded and bolted joints**

228 The tests on the connections between the various elements were of different types: extensive visual inspection,
229 removal of bolts and nuts from bolted joints of the deck, and in-situ investigations of bolted and welded joints with
230 combined visual, magnetic and ultrasound methods.

231 From the visual inspection, many bolts present high states of surface corrosion; the ultrasound investigation
232 extended to the beam-arch connection bolts did not identify breakages or deep cracks in the bolts for shear strength.
233 Instead some nuts and the heads of some bolts were affected by the oxidation layer with exfoliation, generally
234 superficial and not deep.

235 Considering that the nominal tensile strength of a class 10.9 bolt is $f_t = 1000$ MPa, the results obtained by direct
236 and indirect tests can be acceptable and compatible with the design strength class.

237 Furthermore, bolts of the arch-beam joint were tested through ultrasounds: the length of each bolt was equal to an
238 average of 157 mm and no internal defects were observed, after eliminating the surface area damaged by corrosion.

239 It therefore seems possible to preserve the existing bolts after cleaning with sandblasting to white metal and
240 creating a new layer of protection, without altering its functionality.

241 No significant defects were found on the welded continuity joints of steel arch and principal beam, confirming the
242 results of the tests on the original welds already available in the original documentation.

243 About bars and couplers of hangers, the investigations were carried out in-situ with a magnetic method and
244 ultrasounds in several sample points. In this case, three types of joint are distinguished:

245 a) the lower junction of the hanger welded to the web of the main beam (fig. 3c);

246 b) the upper joint of the hanger welded to the connection plate to the arch box (fig 3a,b);

247 c) the coupler joint with welds between the coupler and the bar of the hanger (fig. 4).

248 In the lower junction of the type (a) there were many surface defects due to the high degree of corrosion with some
249 cracks, mostly superficial. No deep cracks emerged that seem to compromise the tightness of the joint.

250 For the upper joint of type (b) there were surface defects and advanced corrosion in some upper plates, especially
251 in the lower area of the connection (lower point of attachment between the hanger bar and the connection plate)
252 with exfoliation and deep incision of the weld due to oxidation. The tightness of some connections is therefore to
253 be considered compromised.

254 For the joint of type (c) between the hanger and the coupler, very significant defects were found due to the
255 extremely high state of corrosion, especially in the upper attachment areas of the coupler, with exfoliation of the
256 coupler body, fractures on the welds and reduction of the cross-section at the attachment of the hanger bar. This
257 situation made it impossible to carry out an internal investigation of the welds, since cleaning with sandblasting
258 would be necessary before reaching the still effective area. As a result, many coupler joints are limited in
259 functionality and unreliable.

260 From the analyses it can be concluded that while the joints of the hanger with the deck beam, although corroded,
261 are not of particular concern, the situation of the joints at the top of the hanger with the arch and the coupler joints
262 are to be considered damaged by corrosion with some elements that cause particular concern for the joint strength.

263 In addition, at the base of the hanger high corrosion damage is located when the hanger passes through the hole in
264 the beam upper flange.

265 **2.1.5 Chemical and metallographic analyses**

266 Chemical and metallographic analyses under the microscope were carried out on different elements, aimed at
267 identifying the chemical composition of the steel used for construction and the analysis of the crystalline structure
268 of the steel as well as the stratigraphy of the coating. The samples are intact without significant corrosion.

269 It should be noted that the percentages of carbon, silicon, phosphorus and sulfur are lower than those declared in
270 the sheet metal alone tested during the works, while the percentage of manganese appears comparable. In
271 particular, the reduced amount of carbon and silicon can influence the mechanical characteristics of both strength
272 and hardness of steel, since the reduced percentage of carbon is generally responsible for reduced tensile strength,
273 such as that found by the strength tests carried out.

274

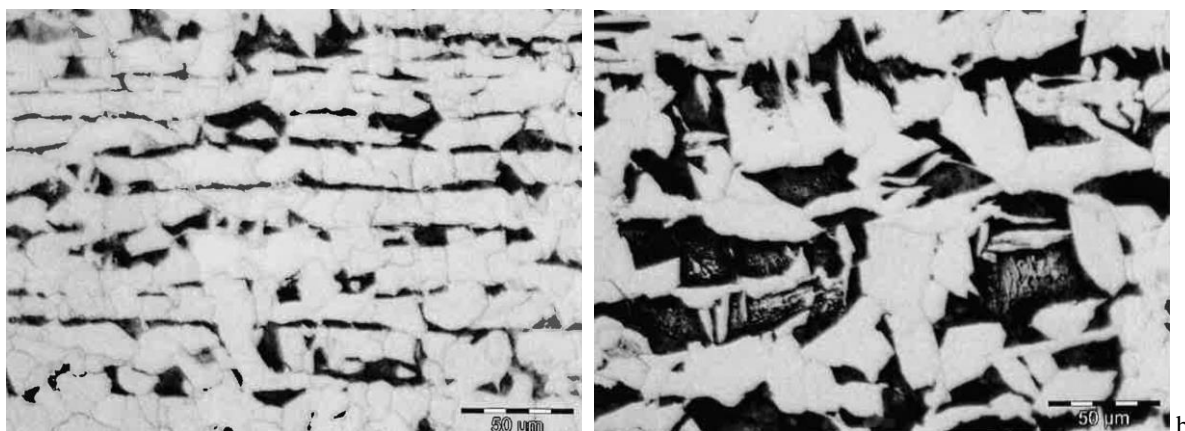
Sample	%Fe	%C	%Si	%Mn	%P	%S
W1	98.15	0.1185	0.1863	1.807	0.0111	0.0098
W2	98.04	0.1363	0.1861	1.122	0	0.0007
W3	98.10	0.1393	0.2414	1.356	0	0
W4	98.15	0.1879	0.1628	1.333	0	0
Average of in-situ tests	98.11	0.1455	0.1942	1.4045	0.0028	0.0026
Original steel tests	98.10	0.1930	0.2450	1.4350	0.0215	0.0120

275 *Table 1. Chemical analysis of steel samples*

276

277 Metallographic analyses were carried out under the microscope on the four in-situ samples. Samples W1, W2 and
278 W3 appear with ordered structure without defects and with medium-sized grains. Samples W2 and W3 show a
279 band structure typical of structural elements with hot laminated steel, with longitudinal arrangement of the pearlite.
280 From the metallographic point of view, the samples have comparable characteristics in the distribution of pearlite
281 within the ferritic matrix. Sample W4 (taken from the deck steel beam) has a larger size and quantity of pearlite
282 grains than the other samples. The strength and hardness of this steel were higher than the others, as was the
283 percentage of carbon. From the comparison it can be said that the steel used for the main beam is different from
284 that used for the other elements. The best results provided by the mechanical tests on sample W4 (deck beam)
285 seem to be confirmed by the metallographic analyses (fig. 7); comparison of the metallographic analyses, strength,
286 hardness and chemical compositions seems to assign a reduced mechanical performance to the other elements, in
287 line with the onsite investigations.

288



289 a
290 *Figure 7. Metallographic views under the microscope (500X). a) steel with minor size of pearlite grains; b) steel*
291 *with major grains and best strength properties*
292

2.2 Dynamic investigation

Dynamic tests were carried out on 7 different hangers. They were investigated by means of three accelerometers located at 1/6, 2/6 and 3/6 of the length in the perpendicular direction to the arch plane (transverse y direction) for identifying the modal shape and frequencies. On some hangers the test was also repeated in an orthogonal direction to the hanger but on the arch plane (global x direction), in order to verify the geometric symmetry and the constraint degree to arch and deck beam.

The characteristic behavior of the hanger, consisting of a 70 mm diameter steel bar, is that of showing the equal importance of the bending (beam) behavior and the typical axial behavior of the tie rod. For this reason, the theoretical research of the modal frequencies cannot rely on the usual equations of the beam or vibrating string, since the frequencies that depend on flexural inertia and axial force are different from those of a rope or a flexional stiff beam. Hence the comparison of the frequencies obtained by onsite investigations must be carried out with the results of the fourth-order differential equation which governs the problem of the dynamics of elements having a bending and axial stiffness and subjected to a significant axial force, which modifies the vibrational characteristics [11,12].

The equation which governs the problem is the following one:

$$T \frac{\partial^2 y}{\partial x^2} - ESj^2 \frac{\partial^4 y}{\partial x^4} = \rho S \frac{\partial^2 y}{\partial t^2} \quad (1)$$

where j is the radius of inertia, ρ is the mass per unit of volume, S the cross section area, (ρS the mass per unit length), E is the elastic modulus and T the value of axial force.

Since the numerical resolution of eq. (1) and identification of the eigenvalues is rather complex [13], approximate solutions have been developed in the literature, for which the n^{th} modal frequency is given by the relationship [14]:

$$f_n = \frac{n}{L} \sqrt{\frac{T}{\rho S} \left(1 + 2 \sqrt{\frac{ESj^2}{TL^2}} \right)} \quad (2)$$

where L is the length of the element, in the case of clamped ends.

A comparison of the frequencies found by eq. 2 was made with those found through an FE model of the hangers carried out in the software MIDAS Gen 2019, applying an initial prestress through the specific function of the software for determining the modal frequencies; this function gives an FE solution of eq. 1 to the specific case of boundary conditions. In fact the free length is here reduced of about 50 cm with respect to the overall length because of the connection welded to the deck beam and, at the hanger top, to the arch, as well as the passage from the hole of the beam flange at the base of the hanger. This modifies the constraint conditions: a clamp is approached in the x direction (longitudinal direction) while an intermediate behavior between clamp and hinge is registered in the y direction (transverse direction).

Since in eq. 2 the value of the axial force is an important variable to be known a priori, the value T introduced into the equation is the one determined through the global bridge model already carried out

327 in the Finite Element software. The comparison between the results of onsite tests and the theoretical-
 328 numerical elaborations is reported in table 2 for the first modal frequency and in table 3 for the second
 329 one.

330

Hanger	Axial force T	L	Theoretical frequency	FE half clamp	FE clamp	Experimental frequency	Deviation
	kN	m	Hz	Hz	Hz	Hz	
08 M	232.7	12.65	3.99	3.87	4.24	3.66	-5.426%
09 M	223.5	13.50	3.65	3.53	3.86	3.70	1.370%
09 M dir. X	223.5	13.50	3.65	3.53	3.86	3.70	1.370%
13 M	206.3	15.30	3.06	2.96	3.21	3.17	-1.246%
13 M dir. X	206.3	15.30	3.06	2.96	3.21	3.32	3.427%
19 M	223.5	13.50	3.65	3.53	3.86	3.30	-6.516%
09 V	223.5	13.50	3.65	3.53	3.86	3.70	1.370%
14 V	206.0	15.40	3.03	2.94	3.18	2.90	-1.361%
14 V dir. X	206.0	15.40	3.03	2.94	3.18	3.10	-2.516%
22 V	269.0	10.40	5.32	5.16	5.74	5.30	-0.376%

331 *Table 2. First modal frequency of hangers*

332

Hanger	Axial force T	L	Theoretical frequency	FE half clamp	FE clamp	Experimental frequency	Deviation
	N	m	Hz	Hz	Hz	Hz	
08 M	232.7	12.65	7.99	8.42	9.20	7.76	-2.879%
09 M	223.5	13.50	7.29	7.65	8.33	-	-
13 M	206.3	15.30	6.11	6.34	6.85	6.54	3.155%
13 M dir. X	206.3	15.30	6.11	6.34	6.85	6.84	-0.146%
19 M	223.5	13.50	7.29	7.65	8.33	6.90	-5.350%
09 V	223.5	13.50	7.29	7.65	8.33	7.80	1.961%
14 V	206.0	15.40	6.06	6.29	6.79	6.25	-0.636%
14 V dir. X	206.0	15.40	6.06	6.29	6.79	6.35	0.954%
22 V	269.0	10.40	10.64	11.45	12.64	-	-

333 *Table 3. Second modal frequency of hangers*

334

335 The results show good agreement between the theoretical value of the frequencies of the 1st and 2nd
 336 modes and what is determined by onsite tests. The comparison between the theoretical values of
 337 frequencies and those obtained by the FE model allowed the author to calibrate the FE model and to
 338 consider it reliable for the evaluation of tensile axial forces of hangers due to dead loads. The greatest
 339 deviation (in reduction) shown by hangers 19 M and 08 M can be attributed to different factors:

- 340 - a different value of axial force in that hanger, different with respect to the theoretical one (which
 341 would lead to a lack of homogeneity in the distribution of the hanger tensions and therefore in
 342 the actual behavior);
- 343 - a different constraint condition with reduction of stiffness at the ends (which would result in
 344 less functionality of the end welded connections);
- 345 - a concentrated lack of stiffness due to the coupler condition (which would lead to damage to the
 346 coupler with reduced functionality).

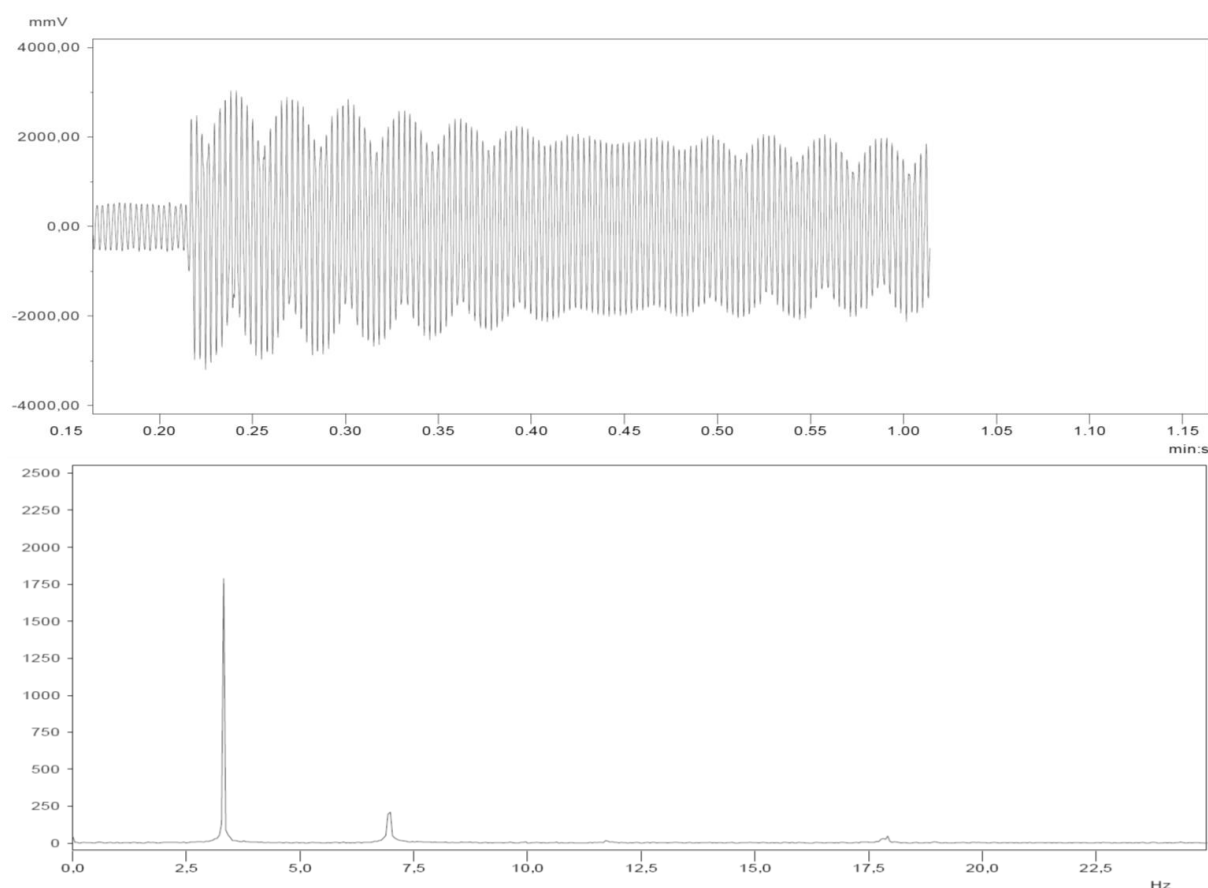
347 Particular attention should be paid to hanger 19M because the reduction deviation is strong on both the

348 two frequencies and also with respect to the symmetrical 09M and 09V hangers, which have higher
349 frequencies, in line with those determined by the theoretical-numerical evaluations. This implies an
350 asymmetry of behavior on both the bridge sides to be attributed to possible reductions in tension or
351 stiffness of the hanger constraints with respect to the symmetrical ones. Figure 8 shows the typical result
352 of a dynamic analysis on a hanger.

353 The dynamic tests on the deck were later repeated, placing three accelerometers at 1/6, 2/6 and 3/6 of
354 the deck span, on the edge of the principal beam. The measurement was carried out in the z direction
355 (orthogonal to the road surface) and the excitement was given through the jerk of a truck obtained with
356 the introduction of an artificial bump in the middle of the bridge. The measurements confirmed a value
357 of the first modal frequency, on both occasions, equal to approximately 1.8 Hz. The value obtained was
358 compared with the theoretical model, with very good agreement.

359 Considering the excited mass and the overall result of the frequencies recognized with onsite tests it is
360 believed to be possible to validate the FE model of the bridge and to consider the values obtained
361 acceptable.

362
363



364

365
366
367

Figure 8. Dynamic tests on hangers: oscillography and analysis in the frequency domain

368
369

2.3 Conclusions of investigations and test analysis

From the results of onsite investigations and laboratory tests, from the correlations between direct and indirect measurements, from the investigations on the welded and bolted connections and from the comparisons with the original data of construction, it can be concluded that:

a) the chemical and mechanical characteristics of the steel used for most of the structural elements do not coincide with those declared in the original documentation; in particular the mechanical characteristics of the steel are lower than those of S355 grade and near those of S275 grade: for this reason the latter one was the strength class used for all checks.

b) The high degradation due to corrosion of hangers (reduction of cross-section) obtained from ultrasonic thickness tests, associated with the reduced strength of steel, can lead to a danger of susceptibility to stress peaks for maximum loads and/or fatigue failures.

c) The high corrosion degradation of the welded joints, especially at the top of the hangers (connections to the arch) and at the bar couplers, leads to a partial loss of functionality with the danger of breakage or failure for some hangers due to the tensile axial stress induced by the maximum loads.

d) The thickness of coating in the main elements seems to be adequate for the steel protection but in many points the corrosion under the skin is still in progress as the 2010 maintenance intervention does not seem to have stopped the corrosion in the points of greatest attack due to insufficient cleaning of the support from oxides before applying new layers of paint.

e) The susceptibility to corrosion of the carbon steel used in the marine environment is very high and the protective layer must be improved to increase the durability of the existing elements but it is not possible to preserve the existing hangers because the state of degradation at present is too high, with the danger of local and/or global collapse of elements (in the case of progressive failures) for maximum service loads.

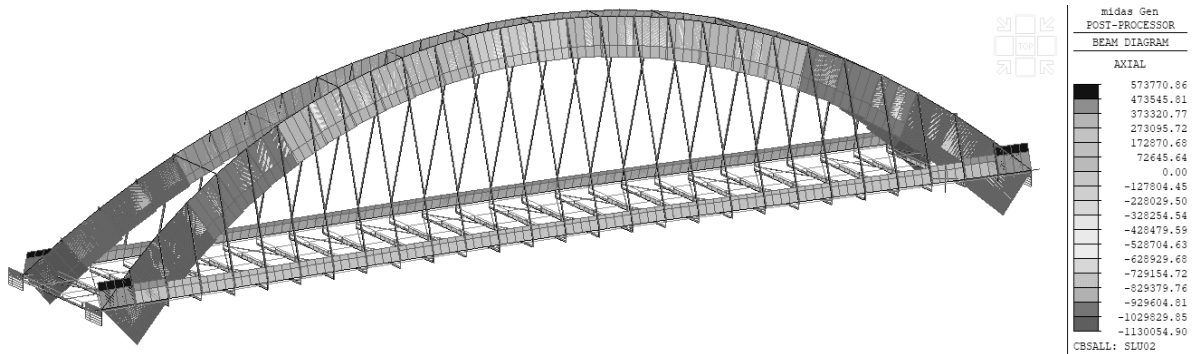
3 Structural evaluations

For the structural analysis, a Finite Element model was carried out using MIDAS Gen 2019 software. The model is three-dimensional, with beam type elements for the steel members and shell type for the deck slab: the full model is composed of 636 joints, 761 beam elements and 112 shell elements. Two analyses were performed: a linear one and a geometric nonlinear one. The results of the two analyses agree with slight differences for the undamaged bridge; for this reason only the results of the linear analysis are shown here. Figure 9 shows the main results of the analysis of the undamaged bridge for the combination of dead load and moving loads. If the bridge was in the ideal undamaged conditions of the original project, all the checks would be satisfied. Unfortunately, the state of degradation due to corrosion of elements does not make it possible to evaluate the global and local safety coefficient with the stress checks; it is also necessary to consider the reduced section of some hangers, heavily damaged by oxidation. Since the reduction of the steel cross-section is not homogeneous on all the hangers and does not show the same extent, it is not possible to hypothesize homogeneous redistribution of the stresses between the elements of the bridge, hence the most important effect is the local one due to stress peaks. The central hangers have been reduced in their section for an average value of 5 mm to 10 mm:

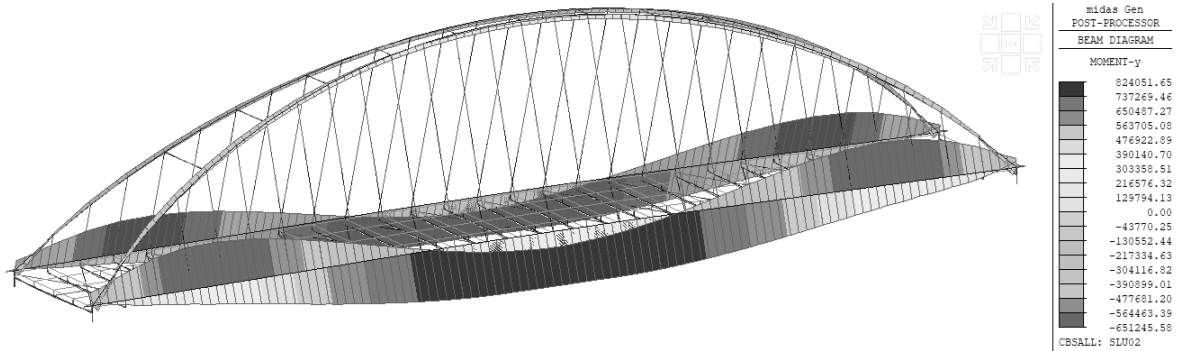
409 i.e. the nominal diameter of 70 mm is reduced to 65 mm and in some cases to about 60 mm.

410

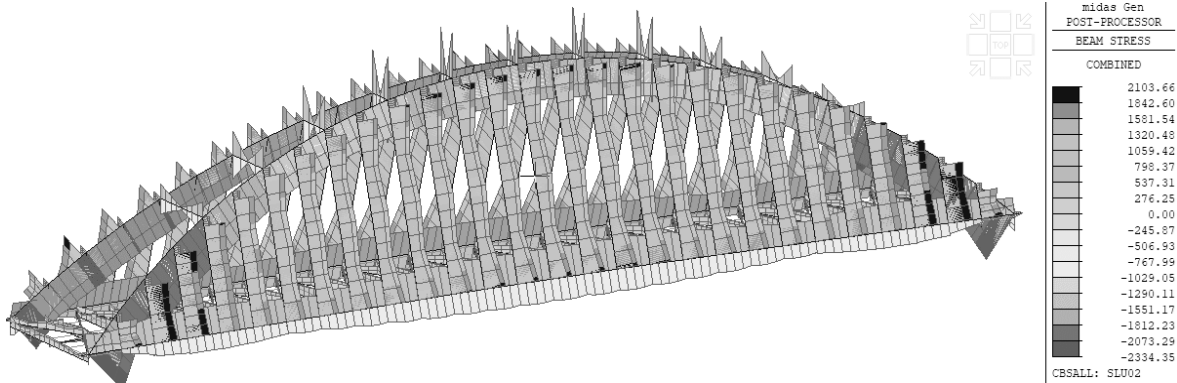
411 a



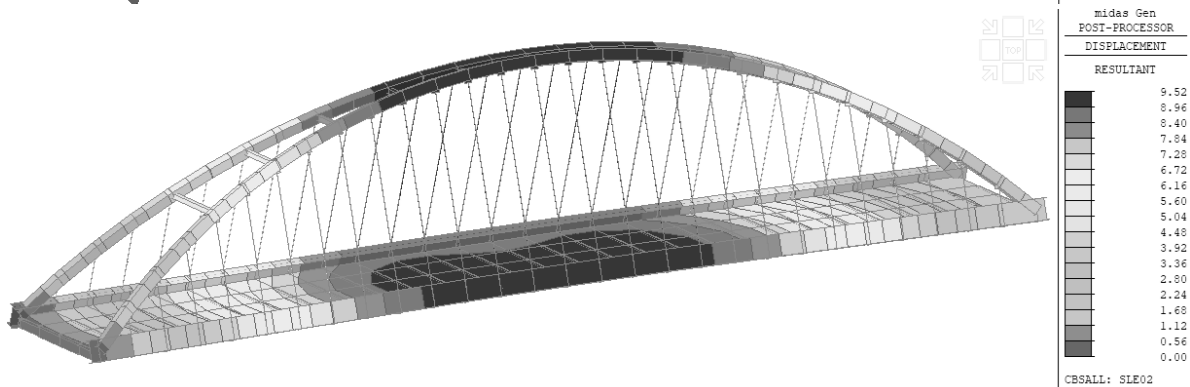
412 b



413 c



414 d



415

416 *Figure 9. Results of FE analysis of the undamaged bridge for dead loads + moving loads. a) Max-min axial*
 417 *force (kN); b) Max-min bending moments(kNm); c) Max-min stress in steel elements (MPa); d) Max*
 418 *displacements (cm)*

419 Therefore, the checks for stress peaks, based on the resultant forces obtained from the FE model that are
 420 to be expected in the hangers, are shown in table 4.

421 Values above 1 for moving load combinations computed according to Eurocode [15] show that the
 422 checks are not satisfied, associated with the steel strength properties obtained by onsite tests. The checks
 423 were carried out with Eurocode provisions [16].

424 If cross-section reduction due to corrosion increases, reaching the diameter of 55 mm, the checks show
 425 the achievement of the ultimate limit state and the danger of local failure for sudden breakage for the
 426 combination of dead loads.

427 For this reason, the bridge is currently subject to limitation of heavy traffic. Further damage due to
 428 corrosion would lead to total closure.

429

HANGER	d	A	J	W	HANGER	d	A	J	W
14V	[cm]	[cm ²]	[cm ⁴]	[cm ³]	18V	[cm]	[cm ²]	[cm ⁴]	[cm ³]
	6.0	28.274	63.61725	21.206		6.0	28.274	63.617	21.206
	Load Combinations					Load Combinations			
FORCES	SLU01	SLU02	SLU06	SLU09	FORCES	SLU01	SLU02	SLU06	SLU09
N [N]	287720	418740	419650	419510	N [N]	303780	438430	438790	439200
M [Ncm]	290240	287650	297480	296570	M [Ncm]	251490	247600	258530	257800
σ [MPa]	238.6	283.7	288.7	288.2	σ [MPa]	226.0	271.8	277.1	276.9
Check σ/f_k	0.9111	1.0834	1.1023	1.1005	Check σ/f_k	0.8630	1.0379	1.0580	1.0573

430 *Table 4. Examples of stress check for two hangers damaged by corrosion. d: diameter, A: area, J: moment of*
 431 *inertia, W: strength modulus*
 432

433 **4 Bridge retrofit: replacement of hangers and corrosion protection**

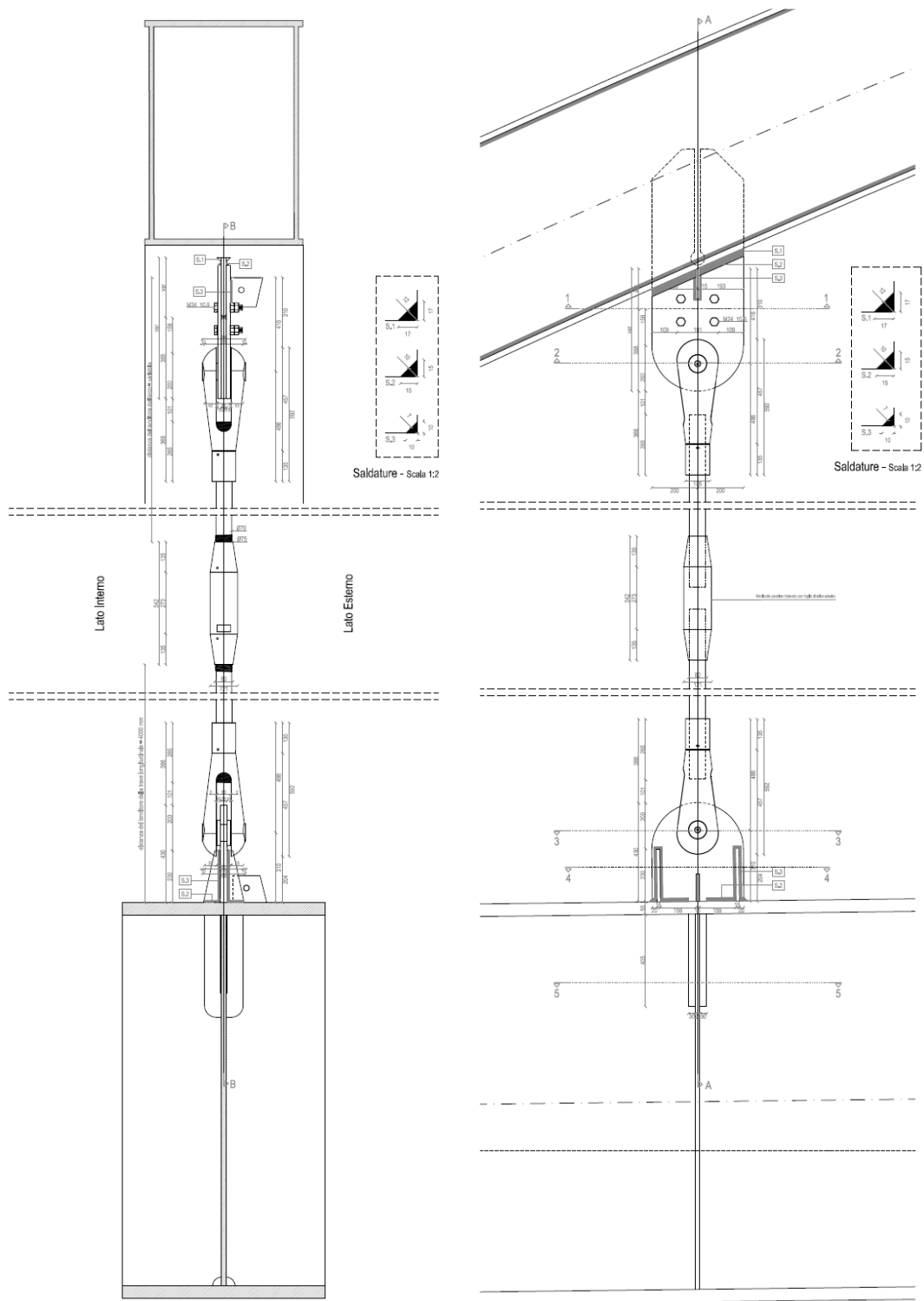
434

435 For the retrofit of the bridge, the most complex intervention is replacing the existing hangers [17]. It is
 436 planned to replace 46 hangers out of the total of 54, maintaining onsite the first two existing hangers on
 437 each side of the bridge. The replacement must take place with adequate supports and retaining tools
 438 (retaining cables, shoring tower, etc.) in order to also replace the anchor joints of the hanger on the arch
 439 and beam. The entire welding area of the hanger to the beam will then be cleaned and the upper plate
 440 anchoring to the arch will be partially cut to make way for the new plates. The hanger, currently
 441 embedded at the ends through the welded connections, will become a hanger-rod with forks and final
 442 pin on both sides (pinned-pinned tie rod), in order to reduce the stress on the end welds. The replacement
 443 will take place for one hanger at a time with a precise sequence, from the ends towards the center of the
 444 bridge both longitudinally and transversely.

445 The existing hanger will be divided into several parts and during cutting stresses and deformations must
 446 be monitored, both on the hanger itself and on the adjacent ones, also evaluating the displacements
 447 induced by the release of the cut hanger. The new hanger will then be assembled, and equipped with a
 448 tensioner for adjusting the axial stress, in order to recover the pre-stress and previous deformed
 449 configuration under dead loads. The whole operation will be monitored with strain gauges on the old

450 and new hangers and with measurement of displacements along the bridge.

451



452

453

454

Figure 10. Geometry of the new hanger

455 Figure 10 shows the geometry of the new hanger. It will be made of a 70-mm diameter bar like the
456 existing one, with hot galvanized steel S355JR type; the intermediate tensioner will be able to adjust the
457 hanger after it has been put into position providing pre-tension that brings the state of stress of the new

458 hanger back to that of the existing one. The aim is not to change the original state of the bridge after the
459 work was completed in 2004, maintaining the states of stress and deformation of the final construction
460 stage.

461 The choice of maintaining the rigid bar like in the original design was taken carefully by the designer
462 under request of the Owner, after checking hanger for fatigue failure following the recommendations of
463 Eurocode. In fact, an hanger made of cables would perform better with regard to deterioration and
464 redundancy, because a crack developed at the surface of the 70-mm bar would grow under fatigue to
465 cause failure of the cross-section of the hanger. Generally the deterioration of a hanger made of high-
466 strength steel wires, would be highly more redundant and perform better under fatigue. However in this
467 case the stress variation was rather low thanks to the small distance between the hangers; furthermore,
468 the choice of creating a pinned-pinned connection made it possible to eliminate the welds at the top and
469 bottom of the hangers, improving their performance also in terms of fatigue. The redundancy is therefore
470 entrusted to the spacing of hangers and to the low value of the service stress.

471 The bar of the new hanger, as well as forks, pins and tensioners, will be hot-dip galvanized in the factory,
472 taking care that the threads undergo effective galvanization to guarantee rubbing strength. The anchor
473 plates will instead be welded and galvanized onsite. All the elements will then be protected with the
474 same painting cycle: high adhesion zinc-based epoxy primer suitable for already galvanized surfaces,
475 high solid epoxy intermediate layer, and white polyurethane finishing layer.

476 It is necessary to insert a Teflon tape around the pin and between the adhering plates for disconnection
477 of the contact between the hot-dip galvanized and the elements galvanized onsite, in order to avoid
478 concentrated corrosive phenomena due to possible dielectric couplings. The same must be done outside
479 the tensioner by sheathing the area of the tensioner and the threads with a Teflon sheet so that the flowing
480 water does not infiltrate the tensioner and localized stagnation and corrosion does not occur.

481 For protection of the existing structures, a sandblasting cycle of SA3 grade, onsite thermal spray
482 galvanization (zinc coating) and subsequent painting cycle are planned. In fact, it is not believed that
483 the owner can rely again exclusively on an epoxy-based cycle, since this has twice proven to be
484 ineffective in the short span of 15 years. Hence a zinc based cycle must be implemented. There are two
485 ways to deal with the problem:

- 486 - one would be to proceed with a "thermal spray zinc" type treatment, used in all English and
487 Norwegian bridges as a rule for over thirty years, as well as in the USA, precisely for steel
488 bridges by the sea [18]. This technology is the safest and best performing, with a high
489 technological level for installation on existing structures.
- 490 - The alternative is to treat the surfaces, after sandblasting and complete cleaning, with a painting
491 cycle that includes a zinc-based primer, also called "cold galvanizing", i.e. pseudo-metallization
492 with a layer of paint with zinc oxide sprayed or brushed on, with high protective thickness and
493 a subsequent layer of epoxy paint only for coverage, for additional protection of the sacrificial
494 layer.

495 In addition to the two galvanizing alternatives, there is the option of the duplex, i.e. a first metallization
496 and a second covering with painting cycle [19]. The choice made in this case is that of duplex technology
497 associated with thermal spray galvanizing and therefore actual in-situ metallization.

498 Thermal spray galvanizing consists in spraying the molten zinc, finely pulverized, on the surface to be
499 suitably protected with sandblasting for white metal (grade SA3). The zinc is sprayed with guns having
500 a melting and spraying device and a zinc feeding device. The fusion is ensured by an electric arc, and
501 the spraying fluid is generally dry and oil-free air, at a pressure of 0.27 / 0.54 MPa. Zinc is used in the
502 form of wire, with a diameter between 1.5 and 2.5 mm. Metallization must be carried out immediately
503 after the preparation of the surface, so that it is still perfectly clean, dry and not oxidized. This is essential
504 for electrical contact and therefore anodic protection of the zinc coating with respect to the steel of the
505 support. The minimum layer of galvanization when finished must be 100 µm. The painting cycle planned
506 after galvanizing is the following.

507 1) Painting with medium-high thickness modified epoxy-polyamide primer with high content of non-
508 toxic active pigments (zinc phosphates) with high adhesion and chemical resistance, particularly suitable
509 for the protection of surfaces of already galvanized steel, and also suitable for retouching welding joints
510 or for repairing damage to the epoxy coating during construction. Quite long recoating intervals with
511 epoxy or polyurethane coatings are possible. It can be covered with a variety of products: chlorinated
512 rubber, alkyd, vinyl, polyurethane, synthetic and oven-baked polyester, epoxy and epoxy. Compatible
513 with cathodic action systems, it has good resistance to water and corrosion. The final thickness of the
514 dry film must be at least 80 microns.

515 2) Painting with two-component, high solid epoxy intermediate layer, formulated with micaceous iron
516 oxides which increases the barrier effect and the long-term protection characteristics of the painting
517 cycle. Used as a high thickness intermediate, it provides excellent barrier protection when used in
518 aggressive environments, such as bridges, chemical plants. The minimum final thickness of the dry film
519 must be 80/100 microns.

520 3) Painting with two-component satin polyurethane enamel, high gloss and surface hardness, which
521 shows excellent resistance to atmospheric agents with the use of an unalterable catalyst. The minimum
522 final thickness of the dry film must be 80/100 microns, and the color white.

523

524 **5 Conclusions**

525 The assessment and retrofit of a steel arch bridge highly damaged by corrosion in a marine environment
526 have been shown and discussed. The results of onsite investigations showed that the steel strength was
527 lower than the expected one and that hangers were the most damaged structural members. Corrosion
528 had reached a very high rate, leading to high level of damage 15 years after construction, in spite of a
529 maintenance intervention already carried out. The lack of galvanized steel in the original project and the

530 ineffective maintenance provided imply that many hangers decrease their serviceability performance till
531 there is a danger of achieving the ultimate limit state in the case of maximum live loads. For this reason
532 it was necessary to design a drastic maintenance intervention with replacement of hangers and
533 sandblasting of all the bridge surface for onsite thermal spray zinc coating and duplex protection through
534 a new cycle of three-layer painting, following the recommendation of American and Northern European
535 Standards. The results of the investigations, assessment and structural analysis are shown, as well as the
536 main intervention planned, in order to give useful tools to engineers dealing with steel bridges in a
537 marine environment.

538

539 **References**

- 540 [1] National Academies of Sciences, Engineering, and Medicine (2013). *Design Guide for Bridges for*
541 *Service Life. Chapter 6 – Corrosion prevention of steel bridges*. Washington, DC: The National
542 Academies Press. <https://doi.org/10.17226/22617>.
- 543 [2] Valdez B., Ramirez J., Eliezer A., Schorr M., Ramos R., Salinas R. (2016), “Corrosion assessment
544 of infrastructure assets in coastal seas”, *Journal of Marine Engineering & Technology*, 15(3), 124–
545 134, DOI:10.1080/20464177.2016.124763
- 546 [3] Alcántara J., De la Fuente D., Chico B., Simancas J., Díaz I., Morcillo M. (2017) “Marine
547 Atmospheric Corrosion of Carbon Steel: A Review”, *Materials (Basel)*, 10(4), 406, doi:
548 10.3390/ma10040406
- 549 [4] Stephens M. T., Gleeson B., Mash J., Li B. (2019) *Steel Bridge Corrosion Prevention and Mitigation*
550 *Strategies. A Literature Review*. University of Pittsburgh, Swanson School of Engineering, IRISE
551 Consortium Impactful Resilient Infrastructure Science and Engineering.
- 552 [5] Kreislova K., Geiplova H. (2012) “Evaluation of corrosion protection of steel bridges”, *Procedia*
553 *Engineering*, 40, 229–234.
- 554 [6] Fernández Troyano L. (2003). *Bridge engineering: A global perspective*, Thomas Telford, London.
- 555 [7] Arici M., Granata M.F., Longo G., Recupero A. (2019) "Conceptual design of bowstring bridges
556 with steel-concrete composite deck", *Proceedings of the International fib Symposium on Conceptual*
557 *Design of Structures*, Torroja Institute, Madrid, Spain - 26-28 september 2019. Edited by: Hugo
558 Corres, Leonardo Todisco, and Corentin Fivet. Fédération Internationale du Béton, 255-262, ISBN:
559 978-2-940643-02-8, ISSN: 2617-4820
- 560 [8] Akpanyung K.V, Loto R.T. (2019) “Pitting corrosion evaluation: a review”, *Journal of Physics:*
561 *Conference Series*, 1378, 022088, IOP Publishing, doi:10.1088/1742-6596/1378/2/022088
- 562 [9] Zhao Y., Zhang Z., Wang G., Li X., Ma J., Chena S., Deng H., Onnis-Hayden A. (2019) “High
563 sulfide production induced by algae decomposition and its potential stimulation to phosphorus
564 mobility in sediment”, *Science of the Total Environment*, 650, 163–172, doi:

565 10.1016/j.scitotenv.2018.09.010

- 566 [10] ASTM (2016). *ASTM A370 / ASME SA-370. Standard Test Methods and Definitions for*
567 *Mechanical Testing of Steel Products*. ASTM International, United States. DOI: 10.1520/A0370-16.
- 568 [11] Gatti P.L., Ferrari V. (1999) *Applied Structural and Mechanical Vibrations. Theory, methods and*
569 *measuring instrumentation*. Taylor and Francis. ISBN 0-419-22710-5
- 570 [12] Clough R.W., Penzien J. (1993) *Dynamics of Structures*. 2nd Edition. McGraw Hill. ISBN 0-07-
571 011394-7
- 572 [13] Lagomarsino S., Calderini C. (2005) “The dynamical identification of the tensile force in ancient
573 tie-rods”, *Engineering Structures*, 27, 846-856, doi:10.1016/j.engstruct.2005.01.008
- 574 [14] Graff K. (1991) *Wave motion in elastic solids*. Cover Publications Inc. ISBN 0-486-66745-6
- 575 [15] European Committee for Standardization (CEN). 2006. *EN 1993-2:2006 Eurocode 3. Design of*
576 *steel structures - Part 2: Steel bridges*, Brussels, Belgium
- 577 [16] European Committee for Standardization (CEN). 2005. *Traffic loads on bridges, part 2. Eurocode*
578 *1*, Brussels, Belgium
- 579 [17] Hayashi T., Ishiyama K., Watanabe, Fujiwara Y., Kumagai Y., Asai, H. (2010). "Renewal of
580 concrete Lohse arch bridge." *Bridge and Foundation Engineering*, 44(9), 49-55.
- 581 [18] Papavinasam S., Attard M., Arseneult B., Revie R. W. (2010) “State-of-the-Art of Thermal Spray
582 Coatings for Corrosion Protection”, *Corrosion Reviews*, 26, Issue 2-3, 105–145, ISSN 2191-0316
- 583 [19] Dallin G., Gagnè M., Goodwin F.E., Pole S. (2018) “Duplex Zinc Coatings for Corrosion Protection
584 of Steel Structures”, *Proceedings of Conference: Transportation Research Board TRB 97th Annual*
585 *Meeting*, January 7-11, Washington, DC, USA.

586

587 **Acknowledgement**

588 Acknowledgement is due to the Owner of the bridge, Libero Consorzio Comunale di Trapani, Sicily,
589 Italy and to the Eng. Patrizia Murana, technical manager of the Owner. Moreover the author thanks
590 to Eng. Michele Infurna and 4EMME Service s.p.a., to Arch. Benedetta Fontana and to all the staff
591 of ICARO PROGETTI Engineering and Architecture.

592